J. Membrane Biol. 143, 177–188 (1995)

The Journal of
Membrane
Biology

Predictive Evidence for a Porin-Type β-Barrel Fold in CHIP28 and other Members of the MIP Family. A Restricted-Pore Model Common to Water Channels and Facilitators

J. Fischbarg, J. Li, M. Cheung, F. Czegledy, P. Iserovich, K. Kuang

Departments of Physiology and Cellular Biophysics, and Ophthalmology, College of Physicians and Surgeons, Columbia University, 630 West 168th Street, New York, N.Y. 10032

Received: 7 June 1994/Revised: 1 September 1994

Abstract. Water channels are the subject of much current attention, as they may be central for cell functions in a host of tissues. We have analyzed the possible fold of facilitators and water channels of the MIP family based on structural predictions, on findings about the topology of CHIP28, and on the biophysical characteristics of water channels. We developed predictions for the following proteins: MIP26, NOD26, GLP, BIB, γ-TIP, FA-CHIP, CHIP28k, WCH-CD1, and CHIP28. We utilized Kyte Doolittle hydrophobicity, Eisenberg's amphiphilicity, Chou-Fasman-Prevelige propensities, and our own Union algorithm. We found that hydrophobic amphiphilic segments likely to be transmembrane were consistently shorter than required for α-helical segments, but of the correct length for β-strands. Turn propensity was high at frequent intervals, consistent with transmembrane β-strands. We propose that these proteins fold as porin-like 16-stranded antiparallel β-barrels. In water channels, from the size of molecules excluded, an extramembrane loop(s) would enter the pore and restrict it to a bottleneck with a width 4 Å $\leq$ w $\leq$ 5 Å. A similar but more mobile loop(s) would act as gate and binding site for the facilitators of the MIP family.

Key words: Membrane proteins — Facilitators — Water channels — MIP protein family — Protein structure prediction

Introduction

Protein water channels through membranes are currently the subject of much interest. Based on their location and distribution (Agre et al., 1993; Hasegawa et al., 1993; Nielsen et al., 1993; Zhang et al., 1993*a*) they may be important for cell volume regulation, for epithelial transport of fluid in general, and for a host of other water movements that take place across cell layers in the lung, blood capillaries, ocular trabecular meshwork, and the like. In past decades, protein water channels were postulated to exist based on indirect but rather compelling evidence (Hays & Leaf, 1962; Solomon, 1968; Macey & Farmer, 1970; Parisi & Bourguet, 1983; Macey, 1984; Verkman, 1992). The strongest evidence for their existence came from the fact that such water channels appeared remarkably specific, permeable only to water and no other small hydrophilic solutes except for formamide (Whittembury et al., 1991). The recent sequencing, cloning, and functional expression of the channel-like integral membrane protein of 28 kDa (CHIP28) water channel (Preston & Agre, 1991; Preston et al., 1992) enhanced the interest in this area, and prompted other laboratories to follow suit. The more recent clonings of several other water channels (Fushimi et al., 1993; Maurel et al., 1993; Zhang et al., 1993*a;* Abrami et al., 1994) have moved the discussion to another level.

Water channels have been reasonably well characterized. Hence, their known properties limit the possible three-dimensional foldings that might otherwise be proposed for their amino acid sequences. We undertook the current analysis to explore their possible structure based on predictive analysis, on initial findings about their topology, and on their characteristic permeability to water and other solutes. We propose that water channels and other members of the MIP (major intrinsic protein of the lens) family of proteins may fold as porin-like β-barrels. Our proposal is meant to help future experimental tests of this and other possible folds for these proteins.

Correspondence to: J. Fischbarg

Materials and Methods

The procedures we used for aligning and predicting protein secondary structures have been detailed before (Fischbarg et al., 1993, 1994). Briefly, we used the Bestfit and Pileup routines of the GCG package (Genetics Computer Group, version 7.0) to perform alignments. We predicted secondary structure using several algorithms: hydropathy, H; Kyte-Doolittle scale, (Kyte & Doolittle, 1982); amphiphilicity, μ; (Eisenberg, Weiss & Terwilliger, 1984); secondary structure propensities (Prevelige & Fasman, 1989); CFP algorithm, for Chou-Fasman-Prevelige; the predictions from a robot that uses evolutionary information in conjunction with a database fed to a neural network (European Molecular Biology Laboratory, Heidelberg, Germany) PHD (Profile network prediction Heidelberg) unmanned server program PHD (Rost & Sander, 1992); and our own Union algorithm (Fischbarg et al., 1993; Fischbarg et al., 1994) that consists in adding hydrophobicity and amphiphilicity propensities, and subtracting CFP 4-point position-dependent turn propensities (pt) for given stretches of proteins. As in the papers above, we scaled H, μ and pt values to −4.5–+4.5, performed algebraic addition, and rescaled the resulting Union propensities to −4.5–+4.5. Three-dimensional molecular modeling was done with the program Hyperchem® (Autodesk, Sausalito, CA) on a 486 computer, and with the program InsightII on a Silicon Graphics platform.

Results

Alignments of CHIP28 with Several other Small Membrane Proteins of Known Structure

We aligned CHIP28 with *Rhodobacter capsulatus* porin (POR1), *Escherichia coli* porin (POR2), the reaction center L chain (RCL), colicin A (COLA), and bacteriorhodopsin (BR), and also aligned POR1 with POR2. The alignments were run with standard GCG parameter values (gap weight = 3.0, length weight = 1.0). The scores (*data not shown*) all fell in a "gray zone" (identity: 19 to 25%; similarity: 44 to 56%). It is well known that bacterial porins are evolutionarily quite distant among themselves, so in spite of the porins having the same secondary structure their sequences show little overall similarity (Welte et al., 1991), and therefore their alignment scores rarely exceed those above. The two porins examined here provided a good example. Hence, a relationship between any two of these proteins can neither be affirmed nor refuted from such values; in particular, whether CHIP28 may fold as either a porin or a multihelical protein cannot be settled by the scores noted.

Multiple Sequence Alignments and Predictions

Figure 1*a* shows a multiple-sequence alignment of nine proteins of the MIP family, namely: (*a*) the major intrinsic protein of the lens (MIP26) (Pisano & Chepelinsky, 1991); (*b*) soybean nodulin 26 (NOD26) (Sandal & Marcker, 1988); (*c*) glycerol facilitator (GLP) (Muramatsu & Mizuno, 1989); (*d*) Drosophila big brain (BIB) (Rao, Jan & Jan, 1990); (*e*) the vacuolar membrane protein (γ-TIP) (Maurel et al., 1993); (*f*) the frog aquaporin (FA-CHIP) (Abrami et al., 1994); (*g*) the proximal tubule water channel (CHIP28k) (Zhang et al., 1993*a*); (*h*) the collecting duct water channel (WCH-CD1) (Fushimi et al., 1993); and (*i*) the erythrocyte water channel (CHIP28) (Preston & Agre, 1991). The similarity between some of these sequences has been pointed out before (Chepelinsky, 1994). However, the last two lines in the alignment of Fig. 1*a* add predictive information arising from the CHIP28 sequence. The last line shows the CHIP28 hydrophobicity profile (for a window of seven residues, and scaled ascendingly from 0 to 9). It is apparent that the regions with higher hydrophobicity, thus presumed to form either α-helical or β-strand structures, correspond to stretches of residues which are reasonably well conserved in the rest of the family. Conversely, the gaps tend to coincide with regions of lower hydrophobicity, and thus presumably forming connecting loops. In line (i), the rectangles label those segments of CHIP28 for which we predict β-structure (*see below*). By and large, they correspond to stretches with relatively higher hydrophobicity and with very few gaps (only in 3 out of the 16 predicted strands). The patterns in Fig. 1*a* are consistent with the existence of secondary structures (α or β) in most hydrophobic segments. This is reinforced by the PHD predictions shown in Fig. 1*b*. To facilitate comparisons, residues occupy the same relative positions in Figs. 1*a* and 1*b*. The PHD algorithm predicts both α-helical and β-strand structures in regions which in Fig. 1*a* are well conserved and hydrophobic. It seems also noteworthy that some homologous segments in a same given region of the alignment are predicted as either α or β depending on the protein examined. This indicates to us that the prediction of a particular type of structure is perhaps less reliable than the prediction that there is secondary α or β structure in a given segment. Assuming hence that there is either type of such structures in the segments delimited by PHD, some of the segments appear too short to span the membrane as α-helices (for which 20 residues are presumed necessary), but have the correct length to span the membrane as β-strands (usually 9–10 residues, but as few as 6 residues may suffice (Radding, 1991)).

Predictions for Membrane Proteins with Known Structure

As we have reported recently (Fischbarg et al., 1994), the conjunction of procedures we utilize gives reasonably accurate predictions of the global fold of those few membrane proteins that have been solved at high resolution so far. We give here an additional evaluation of our procedures in the bar diagram of Fig. 2, which shows the correlation coefficients between predictive procedures and either existing structures, or the predicted structure

of CHIP28. For this purpose, we constructed an arbitrary step function ("structure") valued at 4.5 at existing (or predicted) α or β segments indistinctly, and at −4.5 elsewhere. We verified that smoothing the predicted CFP and Union profiles improved the correlation scores; we chose empirically to smooth the profiles with a fast Fourier Transform filter (span: seven points). As Fig. 2 shows, the Union algorithm correlates better with the correct type of structure in both β-barrel and α-helical proteins (albeit by a narrow margin in the last case, and with understandably large errors given the minimal sample available). CFP overpredicts β structures in the α-helical proteins, although here too the deviations may interfere with the actual picture. On the other hand, CFP correlates better with the structure in the β-barrels; the small error for CFP_β adds credence to it. For CHIP28, Union very narrowly favors β over α structures; however, CFP clearly selects global β folding over α. The difference in favor of the correlation of CFP_β over CFP_α appears too large to be attributed to overprediction.

Predictions for the MIP Family

We applied to the proteins of the MIP family the CFP, PHD and Union predictive algorithms. These results are shown in Figs. 3*a* and 3*b*. For the Union algorithm, we used a span of seven residues; we selected putative angle between residues of 100 and 160 degrees to search for regions with transmembrane α-helix and β-strand propensities, respectively. We also show the corresponding CFP α and β detailed propensities, and the marks for segments that exceed CFP standard thresholds. Lastly, we show the PHD predictions (already given partially in Fig. 1*b*).

We can discern no clear pattern to suggest a multi-α-helical family. In Fig. 3*b*, one can observe some three predicted long segments in the N-terminal half of the proteins. However, the pattern does not seem consistent: depending on which protein is examined, some of those segments break into smaller ones. Even when the U_α propensity is relatively high and maintained throughout the protein, as in MIP26, the CFP_α and PHD marks delimit a fair number of short segments. Even more, in the same MIP26, the U_α profile shows 16 peaks corresponding to comparatively short segments; 16 is the number of β-strands expected from a porin fold. In Fig. 3*b*, the CFP_β marks and the PHD predictions delimit consistent segments which are generally once more too short to span the membrane as α-helices. The U_β profiles exhibit a periodicity consistent with a multistranded β fold. Such patterns are more readily apparent in the N-terminal half of GLP, BIB and γ-TIP, and in the C-terminal half of the water channels. The close correlation of the CFP_β and U_β profiles in the C-terminal half of CHIP28, WCH-CD1 and CHIP28k appears also noteworthy. Turn propensity information is implicit in the U profiles and is not shown in Figs. 3*a* and 3*b* so as not to overload the graphs; still, there are frequent turn propensity markers, all the more so in relatively short proteins such as these. Such high turn propensities are potential structure breakers, so their presence militates against the existence of relatively long, undisturbed segments of helical (α or β) structures. For membrane proteins, this is consistent with the presence of numerous segments of the correct length to be transmembrane β-strands.

CHIP28

Fig. 4 presents in detail predictions for CHIP28, along with marks for the nature of some residues, alignments, and mutation sites. The top panel shows hydrophobicity profiles with spans of 21 and 7. In several instances, where the longer span finds one long hydrophobic segment, the shorter span contains a hint that such segments may be interrupted. The CF turn propensity plot and the marks for segments with suprathreshold turn propensity predict possible turns in regions for which H_{21} would predict a continuous segment. This panel also shows the prior prediction for CHIP28 by Preston and Agre (1991); the alphabetic nomenclature was used for predicted loops.

Immediately above are the marks for our current prediction for β-strands. By comparing such marks to the turn propensity plot, it may be noted how in several cases the putative β-strands coincide with segments relatively devoid of turn propensity, and are "nested" between two flanking turn peaks.

The next two panels show CFP and Union algorithms predicting α and β structures, respectively. Both predict segments that tend to be too short to form transmembrane α-helices. For comparison, our prediction for β-strands is also given in each case. As can be seen, our predictions follow closely the pattern suggested by the CFP_β and U_β profiles, especially in the C-terminal half.

In the bottom panel, we compare how the predicted segments arising from several procedures are aligned. Symbols at top and bottom mark the locations of charged (top) and aromatic (bottom) residues. The PHD, CFα, CFβ, and our own prediction marks are repeated here. The marks for POR1 and POR2 represent the segments of CHIP28 that align with the β-strands segments of each respective porin. The x marks denote sites of recently performed mutations (Preston et al., 1994) (labeled at the bottom).

Prediction Method

We first determined the approximate location of the structured segments, and then refined their lengths using a combination of approaches. One of them was a rule

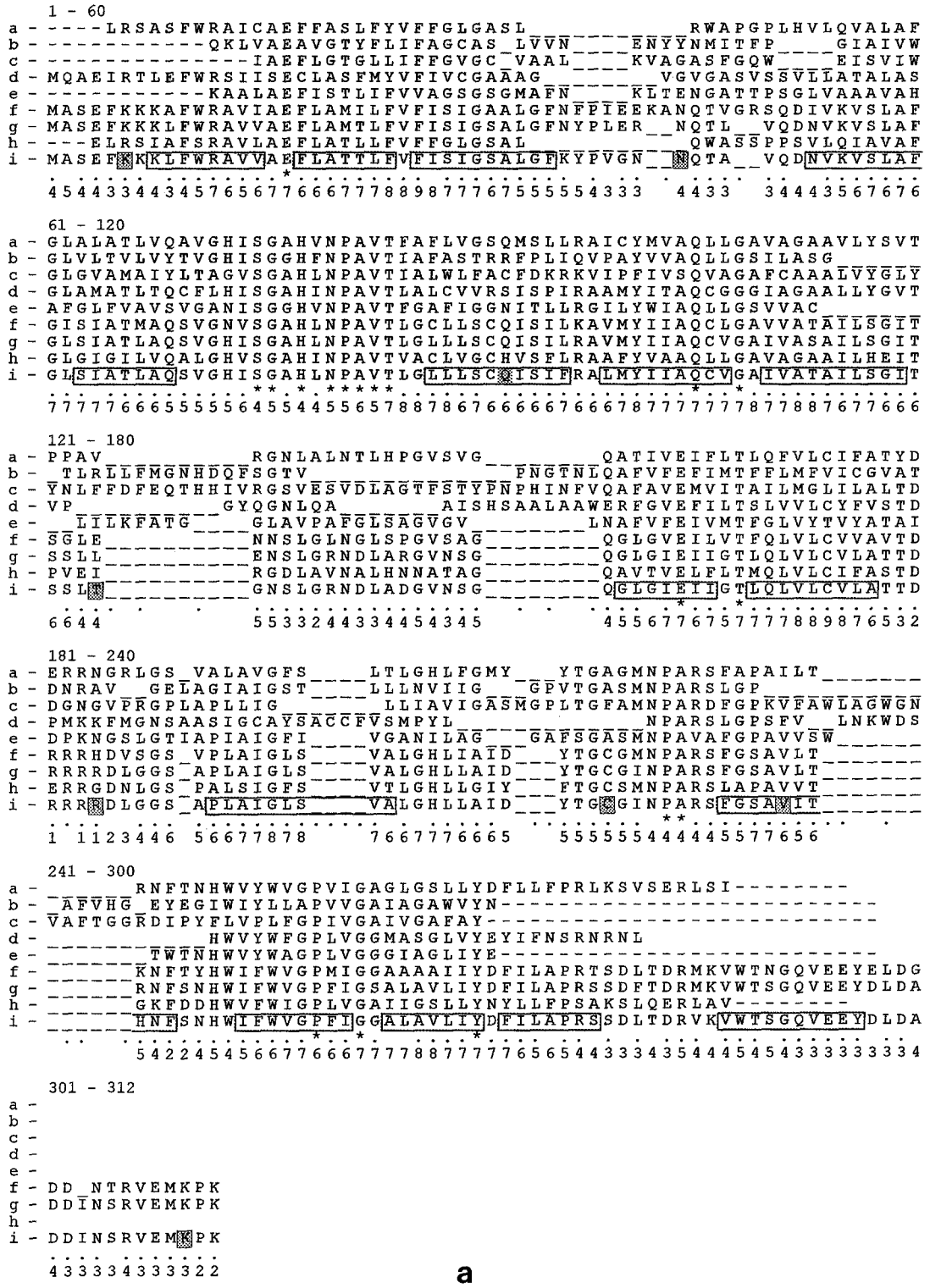

Fig. 1 (*a*) Multiple sequence alignment of the MIP family. Alphabetic identifiers for each protein are detailed in the text. Next to last line: gaps, .: similarity, *: identity. Last line: CHIP28 KD hydrophobicity, span 7, scaled 0-9. Rectangles enclose β-strands predicted here for CHIP28 (*see* Figs. 4 and 5). Stippled rectangles mark sites of mutations done in CHIP28 by Preston et al. (1994). (*b*) PHD predictions for the proteins of the MIP family. Protein identifiers and residue locations as in Fig. 1*a*. @: α-helices; ^: β-strands; -: coils. Blank spaces denote gaps in the alignment.

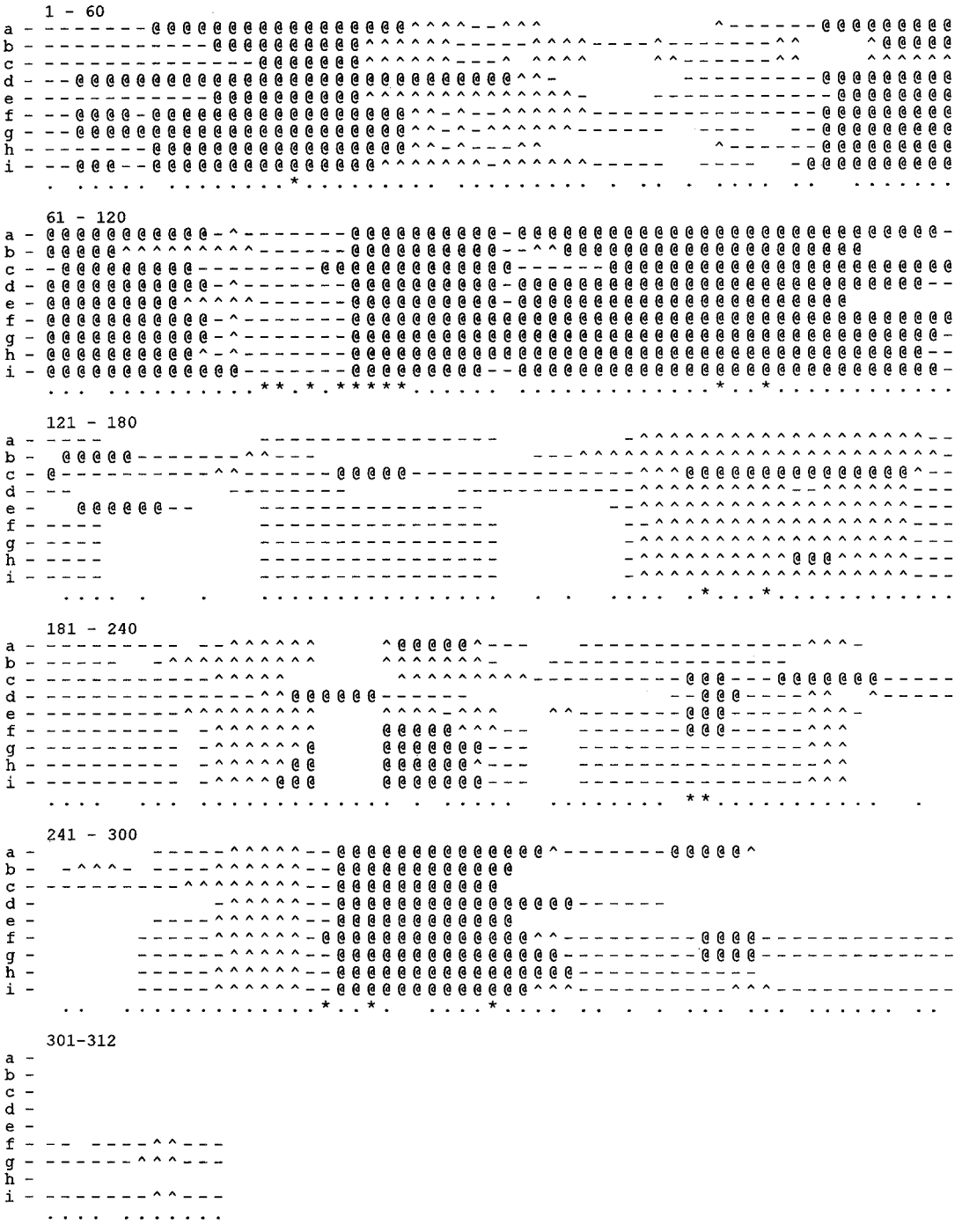

b

Fig. 1. Continued.

derived from porins, namely, that aromatic residues tend to occupy the first position at the beginning or end of a given strand (Cowan & Rosenbusch, 1994). In addition, we sought to place charged residues immediately outside the membrane, where they would interact with the negative phospholipid head groups in the bilayer or with cations associated with them (Cowan et al., 1992). Other criteria were the turn propensities, the length of segments delimited by β marks, and the propensity of given residues to break or cap β-strands.

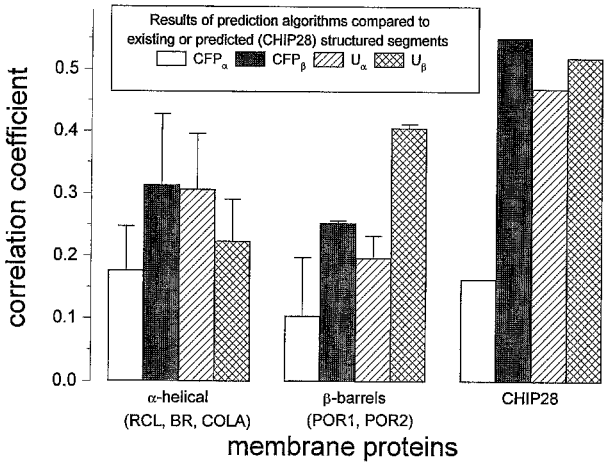

Fig. 2. Averages and SEM deviations for the correlations between predicted and actual high-resolution structures. For CHIP28, in the absence of a structure, we used the β-strand segments we currently predict (*see* Fig. 4).

The assignments of Fig. 4 were reached by dividing the chain in convenient stretches.

Segment 6-42

Mutations locate K6 inside the cells and N42 outside, hence an odd number of membrane crossings ought to exist for the segment between them. H21 has only one peak, but H7 has three. Uα is unclear, but CFPα, CFPβ and Uβ mark three segments, and so does PHD. In the porin alignments, POR1 marks three segments and POR2 two. From this picture, we extract a consensus of three segments. We mark their lengths selecting flanking aromatics for strands 2 and 3, and choose the CFPβ mark to delimit strand 1. Although this last maneuver places charged residues inside strand 1, this does not appear unwarranted since porins (*not shown*) have a fair number of charged residues in structured segments.

Segment 43-70

H21 shows one peak, H7 two, and there is a subthreshold turn at about residue 55. CFPα, Uα, CFPβ and Uβ mark two segments. POR1 and POR2 mark one and two segments, respectively. We note that the pair of CFPβ and Uβ peaks appears well delimited, and opt for marking two β-strands (4 and 5). Segment 60–70 appears hydrophilic and with high turn propensity, so we resume at residue 71.

Segment 71-120

H21 marks one segment, and H7 two. However, there are three turn marks in this stretch. CFPα and Uα mark three segments; the pattern of CFPβ and Uβ is consistent with three segments. The POR1 alignment also shows three segments, so we opt for marking three β-strands (6, 7 and 8). This leaves T120 in an inside loop, in contradiction with the outside placement deduced for it by mutagenesis (Preston et al., 1994). Next comes a hydrophilic region ("loop C") which may have a short α-helical structure, judging from Uα and CFPα. We resume the analysis at residue 135.

Segment 135-155

H21 shows one peak, but H7 has two. CFPα marks two segments, and the Uα peak is consistent with two segments. The CFPβ pattern is consistent with two peaks, and Uβ marks two segments. Both porin alignments mark two segments in this region. We mark two β-strands (9 and 10), which make the end of strand 10 intracellular, back in register with the intracellular location deduced for R162 by mutagenesis (Preston et al., 1994). The next stretch up to residue 165 appears a hydrophilic loop.

Segment 165-189

C189 is in all likelihood extracellular, the site of action of external mercurial inhibitors on water permeation (Van Hoek & Verkman, 1992; Preston et al., 1993; Zhang et al., 1993*a,b*). This requires an odd number of crossings for this segment. There is no clear evidence from any of the algorithms for more than one segment; the porin alignments also mark at most one segment. We mark one β-strand (11) and position it in the region where the Uβ peak is highest and there is a limiting CFPβ mark.

Segment 170-267

Since there is evidence that the C-terminal end is intracellular, as evidenced by the K267 mutation (Preston et al., 1994), this segment is predicted to have an odd number of crossings. H21 shows one peak, H7 three. The CFPα and Uα patterns are unclear, pointing to between three and seven segments. On the other hand, CFPβ and Uβ are remarkably well correlated with each other. CFPβ marks five segments, and Uβ six. The POR1 alignment marks six segments, and POR2 four. We hence extract a consensus for five segments. To mark β-strands 12–15, we select the four regions for which the CFPβ and Uβ peaks are in coincidence. Strand 15 is marked using the turn profile, the Uβ peak centered on residue 254, and the POR1 alignment mark for a β-strand in that region.

In closing this section, it seems worth noting the presence of stretches of residues with charges of opposite signs in close proximity (segments 4–6, 48–51, 126–131, 158–163, 234–243, and 263–269). We discuss below

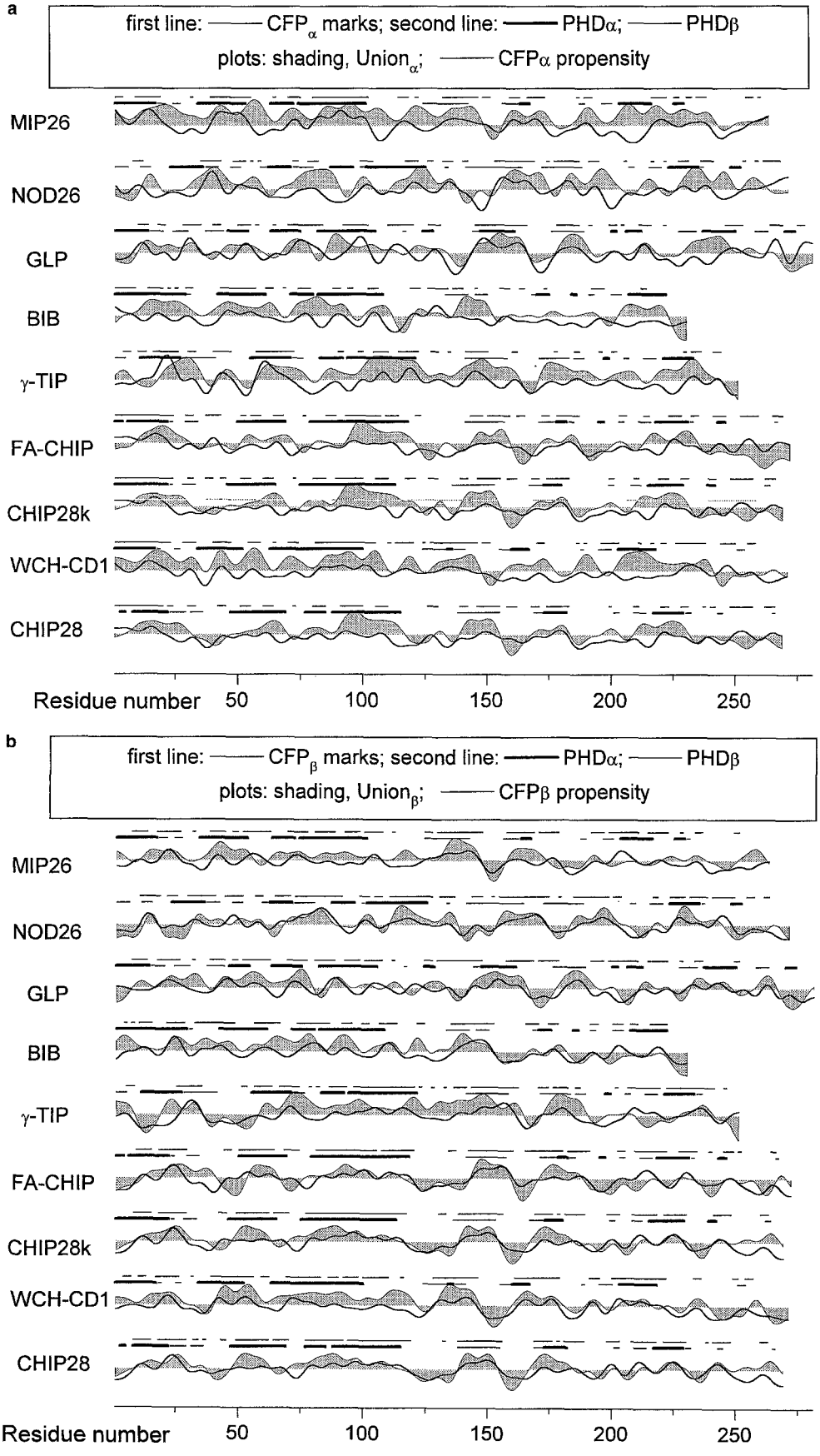

Fig. 3 (*a*) PHD predictions, and Chou-Fasman-Prevelige and Union propensities for all nine MIP family members examining propensity for α structure. (*b*) As in (*a*) but examining propensity for β structure.

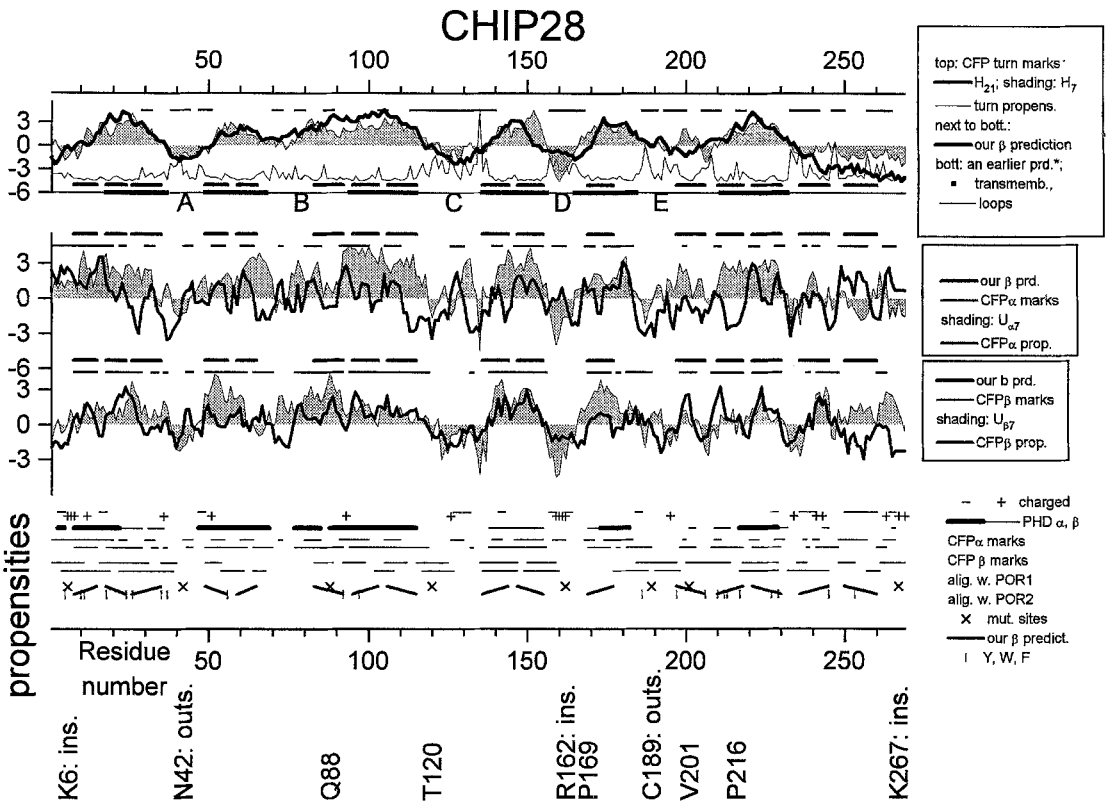

Fig. 4. Detailed analysis of predictions for CHIP28 along with a comparison with results from recent mutations/additions (Preston et al., 1994) of an epitope from the coronavirus E1 glycoprotein. *An earlier prediction (Preston & Agre, 1991).

how these may be related to electrostatic filtering to exclude electrolytes. The topology for CHIP28 suggested in Fig. 4 is given in more detail in Fig. 5.

A CHIP28 Model with a β-Barrel Porin Fold

We displayed graphically *R. capsulatus* porin (*data not shown*) and verified that replacement of individual porin residues in its β-strands by the CHIP28 residues we predicted to be in the corresponding strands did not disturb the H-bonded patterns of the barrel. The predictions above for CHIP28 include a number of loops, so that one or more of them might enter the pore, restrict it as in porins (*see below*), and help confer CHIP28 its particular selectivity for water.

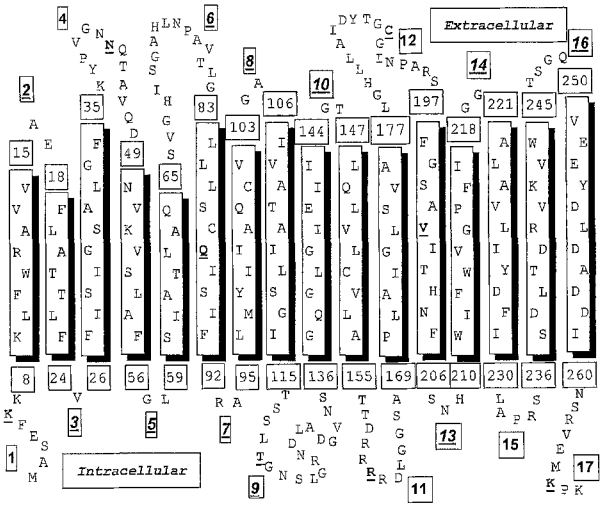

Fig. 5. Our assignments for residue locations in β-strands (vertical rectangles) and in connecting loops of CHIP28. Residue numbers at the ends of each β-strand are given in the flanking legends. Bold legends number the loops; underlining (or the lack of it) marks the loops for which its putative intracellular or extracellular locations disagree (or agree) with those proposed in the earlier model. Residues at mutation sites are bold and underlined.

Evidence for α and β Structures in CHIP28

From CD and FTIR spectroscopy, CHIP28 has been reported to contain roughly equal amounts of α and β structures, 40 and 43%, respectively (Van Hoek et al., 1993). This might be consistent with a type of fold still not found in membrane proteins, the α-β barrel. To look into this, we selected triose phosphate isomerase (TIM), a typical α-β barrel protein of a molecular weight (26.5

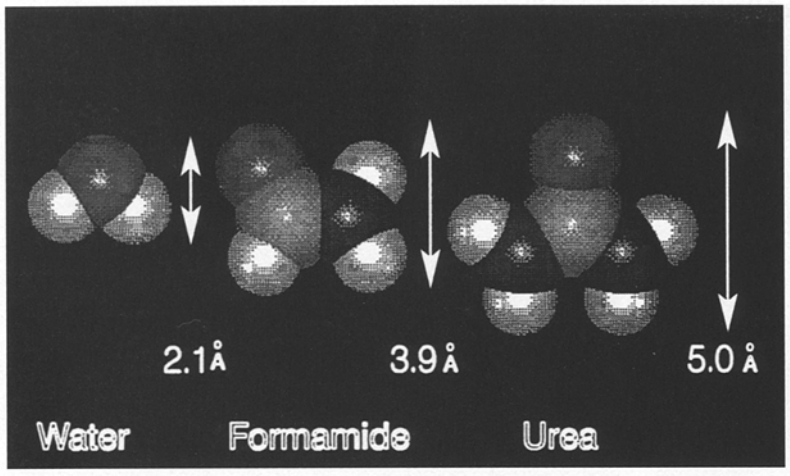

Fig. 6. Space-filling models to compare the dimensions (indicated) that would be key for the given molecules to clear (or not) the postulated channel bottleneck.

kD) similar to that of CHIP28. TIM cannot be said to include a hydrated channel; the diameter of its 8-stranded β-barrel is too small for the purpose and is filled with tightly packed side chains from the strands (*data not shown*). To form a channel, another α-β barrel protein would have to have either more numerous strands or a different sequence and fold; whether such a fold exists is not currently known. In terms of our proposal, an alternative explanation for the CD and FTIR data is that the extramembrane loops may form some α-helices. Whether the amount of α structure thus generated may be enough to correspond to the CD and FTIR data is unclear.

Discussion

β-Barrel vs. Multi-α-Helical Folds

Since the structured transmembrane segments we predict are too short to be α-helices but have the correct length for β-strands, we favor a β-barrel fold for CHIP28. We have previously employed prediction methods similar to those utilized here. In the first instance (Fischbarg et al., 1993), the $U_{\beta 7}$ peaks identified the approximate location and length of the β-strands in two porins. More recently, we have generated similar predictions for other membrane proteins (Fischbarg et al., 1994), including a short description of a putative multi-β-fold for CHIP28. As mentioned above, a prediction for the transmembrane and loop regions of CHIP28 has been advanced (Preston & Agre, 1991) by the researchers that cloned it. In that model, the transmembrane segments are all 20 or more residues long, which is consistent with α-helical structure. The topology of such prediction has been recently tested by vectorial proteolysis (Preston et al., 1994). Figure 5 illustrates the β-barrel model we propose. Several of the characteristics are common to both the prior model and ours; both folds have the NH2 and COO terminals intracellular, the region around R162 as an intracellular loop, and the regions around the glycosylation site (N24) and the Hg-sensitive site (C189) as part of extracellular loops. The models diverge for what they termed loops B and E, in parts where we predict β-strands instead. This would explain why their mutations and E1 epitope additions at Q88 and V201 (Preston et al., 1994) led to nonfunctional proteins, since these would have disturbed the channel fold. Agre and colleagues themselves mentioned in their discussion (Preston et al., 1994) that mutations in loops B and E are less tolerated than elsewhere in the CHIP molecule, and that such loops are candidate structures of the pore-forming domains of CHIP and other aquaporins. That would, of course, increase the number of transmembrane segments above the six originally proposed (Preston & Agre, 1991).

Loop C deserves some consideration, since we predict it inside while the original proposal (Preston & Agre, 1991) has it outside. The evidence from protease digestion of CHIP28 plus an E1 insert at T120 locates such loop outside (Preston et al., 1994). However, this discrepancy may be only apparent; for instance, E1 may have somehow modified the protein fold so as to emerge on the outside. To be noted, aside from this aspect, the picture appears cogent so far.

The Pore of Water Channels

The width of the pore of the porin-like β-barrel we propose is comparatively large. For instance, in *R. capsulatus* porin, the pore has an irregular ellipsoidal cross section with axes of some 13 × 10 Å. If the entire width of such a pore would be available for diffusion, large solutes would traverse this channel. In the porin above, a loop enters the pore, remaining in contact with the barrel wall, and restricts the pore opening to a quasi-triangular cross section of some 9 Å in height and 7 Å at

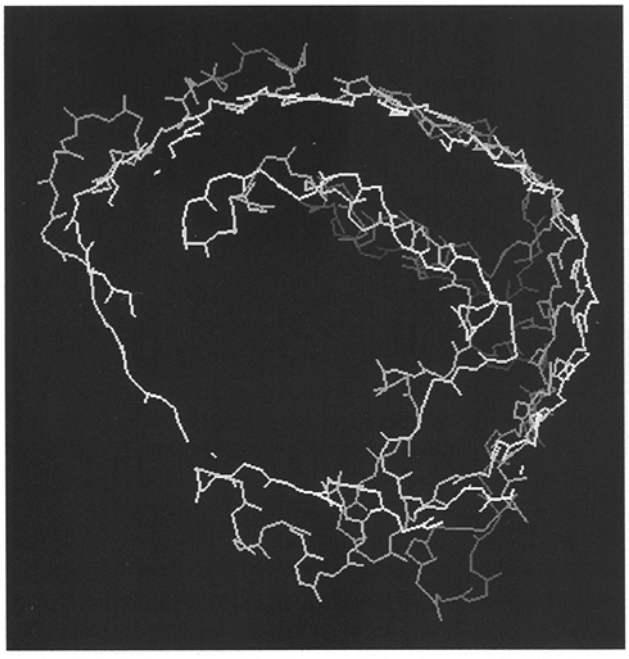

Fig. 7. Cross section of the β-barrel and intrachannel loop of POR1. Only backbone atoms and bonds are shown to allow visualization of the loop disposition.

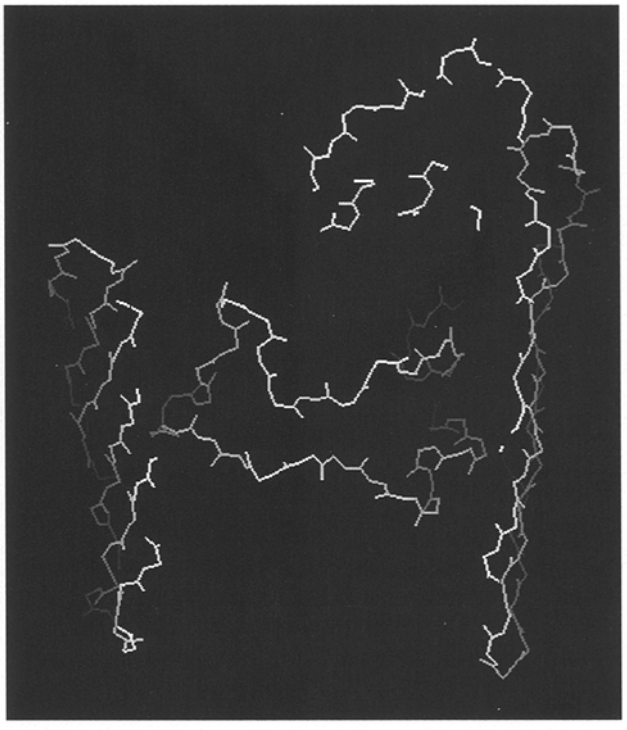

Fig. 8. Longitudinal cross section of a 15-Å slab of POR1 (backbone only).

the base. We are able to propose a barrel model for CHIP28 because it has loops that may restrict the size of the pore, otherwise the model could not be correct. There is evidence that water and formamide traverse a water channel (Whittembury et al., 1991) but not urea (Whittembury et al., 1991; Van Hoek & Verkman, 1992) or compounds larger than it. If so, a steric restriction must exist, and must also be more pronounced than that for porin. From the molecular models illustrated in Fig. 6, the minimum size a pore ought to have for the permeation of these molecules is: for water, 2.1 Å; for formamide, 3.9 Å; and for urea, 5.0 Å. Hence, the loops inside the putative barrel ought to restrict the size of a bottleneck inside the channel to not less than 4 and not more than 5 Å.

As recently reviewed (Agre et al., 1993), CHIP28 does not allow the passage of electrolytes (H+ included). One explanation for this is that the molecule includes one or more electrostatic filters against electrolytes. Such filters could result from the close juxtaposition of charged residues of opposite signs; indeed, some of the predicted loops contain such arrangements, as in segments 126–131 and 158–163.

A Restricted-pore Model for CHIP28 and other MIP Family Members

A model for the MIP family proteins would have to account simultaneously for the large water conductance for water by some of them, and for the facilitator properties uncovered so far for other ones. We propose that a restricted pore such as that found in porins would fit the description. Figures 7, 8 and 9 exemplify this concept by displaying selected views of POR1. Figure 7 shows a cross section of POR1; for clarity, only the backbone appears. As can be seen and as discussed above, one of the loops resides inside its pore and restricts its diameter. The shape of the loop hints at the possible presence of a pocket in its concave site, which might serve to bind substrates in the facilitators. Figure 8 shows a longitudinal section of a 15-Å thick center slab of POR1 (the β-strands in front and in back are not shown for clarity). As can be seen, the restriction created by the loop extends only to a central band rather than to the entire length of the pore. In addition, the loop that appears at the top right might represent an additional binding site or restriction. In Fig. 9, the center of the loop has been removed, and the CPK spheres of the atoms lining the resulting pore are shown so as to give a view of the bottleneck in the pore profile. Parenthetically, the model proposed here differs from one recently advanced by Agre and colleagues (Jung et al., 1994) in that in their case the channel would be circumscribed by two loops, while in the present one the channel is formed by the entire β-barrel translocation unit plus a single loop. As anticipated above, we propose that a fixed barrel framework and a disposition of the loops similar to that of

Fig. 9. As in Fig. 8, except that the center of the loop is not shown and the channel-lining atoms are shown with their space-filling CPK spheres.

porins could account for the selectivity and gating characteristics of MIP family proteins.

Conclusion

As recently reviewed (Cowan & Rosenbusch, 1994), "in the past 10 years detailed structures of a few membrane proteins have so far revealed two folding patterns," meaning multi-α-helical and β-barrel. It is, of course, still unclear whether additional patterns may emerge for integral membrane proteins, but out of the two currently known patterns, the predictions we present favor a β-barrel fold. Clearly work remains ahead before a more definitive model for the proteins of the MIP family can be generated; we hope that our current proposal may provide a useful basis for further experimental tests of their characteristics.

References

Abrami, L., Simon, M., Rousselet, G., Berthonaud, V., Buhler, J.M., Ripoche, P. 1994. Sequence and functional expression of an amphibian water channel, FA-CHIP: a new member of the CHIP family. *Biochim. Biophys. Acta* **1192:**147–151

Agre, P., Preston, G.M., Smith, B.L., Jung, J.S., Raina, S., Moon, C., Guggino, W.B., Nielsen, S. 1993. Aquaporin CHIP: the archetypal molecular water channel. *Am. J. Physiol.* **265:**F463–F476

Chepelinsky, A.B. 1994. The MIP transmembrane channel family. *In:* Handbook of membrane channels: molecular and cellular physiology. C. Peracchia, editor. pp. 413–432. Academic Press, San Diego, CA

Cowan, S.W., Rosenbusch, J.P. 1994. Folding pattern diversity of integral membrane proteins. *Science* **264:**914–916

Cowan, S.W., Shirmer, T., Rummel, G., Steiert, M., Ghosh, R., Pauptit, R.A., Jansonius, J.N., Rosenbusch, J.P. 1992. Crystal structures explain functional properties of two *E. coli* porins. *Nature* **358:**727–733

Eisenberg, D., Weiss, R.M., Terwilliger, T.C. 1984. The hydrophobic moment detects periodicity in protein hydrophobicity. *Proc. Natl. Acad. Sci. USA* **81:**140–144

Fischbarg, J., Cheung, M., Czegledy, F., Li, J., Iserovich, P., Kuang, K., Hubbard, J., Garner, M., Rosen, O.M., Golde, D.W., Vera, J.C. 1993. Evidence that facilitative glucose transporters may fold as beta-barrels. *Proc. Natl. Acad. Sci. USA* **90:**11658–11662

Fischbarg, J., Cheung, M., Li, J., Iserovich, P., Czegledy, F., Kuang, K., Garner, M. 1994. Are most transporters and channels beta barrels? *Mol. Cell. Biochem.* **140:**147–162

Fushimi, K., Uchida, S., Hara, Y., Hirata, Y., Marumo, F., Sasaki, S. 1993. Cloning and expression of apical membrane water channel of rat kidney collecting tubule. *Nature* **361:**549–552

Hasegawa, H., Zhang, R., Dohrman, A., Verkman, A.S. 1993. Tissue-specific expression of mRNA encoding rat kidney water channel CHIP28k by in situ hybridization. *Am. J. Physiol.* **264:**C237–C245

Hays, R.M., Leaf, A. 1962. Studies on the movement of water through the isolated toad bladder and its modification by vasopressin. *J. Gen. Physiol.* **45:**905–919

Jung, J.S., Preston, G.M., Smith, B.L., Guggino, W.B., Agre, P. 1994.

Molecular structure of the water channel through aquaporin CHIP. The hourglass model. *J. Biol. Chem.* **269:**14648–14654

Kyte, J., Doolittle, R.F. 1982. A simple method for displaying the hydropathic character of a protein. *J. Mol. Biol.* **157:**105–132

Macey, R.I. 1984. Transport of water and urea in red blood cells. *Am. J. Physiol.* **246:**C195–C203

Macey, R.I., Farmer, R.E.L. 1970. Inhibition of water and solute permeability in human red cells. *Biochim. Biophys. Acta* **211:**104–106

Maurel, C., Reizer, J., Schroeder, J.I., Chrispeels, M.J. 1993. The vacuolar membrane protein g-TIP creates water specific channels in *Xenopus* oocytes. *The EMBO Journal* **12:**2241–2247

Muramatsu, S., Mizuno, T. 1989. Nucleotide sequence of the region encompassing the glpKF operon and its upstream region containing a bent DNA sequence of *Escherichia coli*. *Nucl. Acids Res.* **17:**4378

Nielsen, S., Smith, B.L., Christensen, E.I., Knepper, M.A., Agre, P. 1993. CHIP28 water channels are localized in constitutively water-permeable segments of the nephron. *J. Cell Biol.* **120:**371–383

Parisi, M., Bourguet, J. 1983. The single-file hypothesis and the water channels induced by antidiuretic hormone. *J. Membrane Biol.* **71**(3):189–193

Pisano, M.M., Chepelinsky, A.B. 1991. Genomic cloning, complete nucleotide sequence, and structure of the human gene encoding the major intrinsic protein (MIP) of the lens. *Genomics* **11:**981–990

Preston, G.M., Agre, P. 1991. Isolation of the cDNA for erythrocyte integral membrane protein of 28 kilodaltons: Member of an ancient channel family. *Proc. Natl. Acad. Sci. USA* **88:**11110–11114

Preston, G.M., Carroll, T.P., Guggino, W.B., Agre, P. 1992. Appearance of water channels in *Xenopus* oocytes expressing red cell CHIP28 protein. *Science* **256:**385–387

Preston, G.M., Jung, J.S., Guggino, W.B., Agre, P. 1993. The mercury-sensitive residue at cysteine 189 in the CHIP28 water channel. *J. Biol. Chem.* **268:**17–20

Preston, G.M., Jung, J.S., Guggino, W.B., Agre, P. 1994. Membrane topology of aquaporin CHIP. Analysis of functional epitope-scanning mutants by vectorial proteolysis. *J. Biol. Chem.* **269:**1668–1673

Prevelige, P., Fasman, G.D. 1989. *In:* Prediction of protein structure and the principles of protein conformation. G.D. Fasman, editor, pp. 391–416. Plenum, New York, London

Radding, W. 1991. Proposed partial beta-structures for lac permease and the Na^+/H^+ antiporter which use similar transport and H^+ coupling mechanism. *J. Theor. Biol.* **150:**239–249

Rao, Y., Jan, L.Y., Jan, Y.N. 1990. Similarity of the product of the Drosophila neurogenic gene big brain to transmembrane channel proteins. *Nature* **345:**163–167

Rost, B., Sander, C. 1992. Jury returns on structure prediction. *Nature* **360:**540

Sandal, N.N., Marcker, K.A. 1988. Soybean nodulin 26 is homologous to the major intrinsic protein of the bovine lens fiber membrane. *Nucl. Acids Res.* **16:**9347

Solomon, A.K. 1968. Characterization of biological membranes by equivalent pores. *J. Gen. Physiol.* **51:**335–364

Van Hoek, A.N., Verkman, A.S. 1992. Functional reconstitution of the isolated erythrocyte water channel CHIP28. *J. Biol. Chem.* **267:**18267–18269

Van Hoek, A.N., Wiener, M., Bicknese, S., Miercke, L., Biwersi, J., Verkman, A.S. 1993. Secondary structure analysis of purified functional CHIP28 water channels by CD and FTIR spectroscopy. *Biochemistry* **32**(44):11847–11856

Verkman, A.S. 1992. Water channels in cell membranes. *Annu. Rev. Physiol.* **54:**97–108

Welte, W., Weiss, M.S., Nestel, U., Weckesser, J., Schiltz, E., Schulz, G.E. 1991. Prediction of the general structure of OmpF and PhoE from the sequence and structure of porin from *Rhodobacter capsulatus*. Orientation of porin in the membrane. *Biochim. Biophys. Acta* **1080:**271–274

Whittembury, G., Echevarría, M., Gutierrez, A., Gonzalez, E. 1991. Contraluminal cell membrane water channels in PST exclude urea and acetamide but are formamide permeable. *J. Am. Soc. Nephrol.* **2:**729

Zhang, R., Skach, W., Hasegawa, H., Van Hoek, A.N., Verkman, A.S. 1993a. Cloning, functional analysis and cell localization of a kidney proximal tubule water transporter homologous to CHIP28. *J. Cell Biol.* **120:**359–369

Zhang, R., van-Hoek, A.N., Biwersi, J., Verkman, A.S. 1993b. A point mutation at cysteine 189 blocks the water permeability of rat kidney water channel CHIP28k. *Biochemistry* **32:**2938–2941